

# Modeling Bose-Einstein condensate with Gross-Pitaevskii equation

Cheng Luo\*

*Department of Physics, Grinnell College, Grinnell, IA 50112*

(Dated: October 13, 2009)

Bose-Einstein condensate is a typical example of a many-body interacting system. This paper derives the nonlinear Gross-Pitaevskii equation that describes BE condensate, and then implements two numeric methods to solve this GP equation. With the mean-field theory, the interatomic interaction can be replaced by a external potential that has the same effect as the interparticle interaction. The interatomic interaction affects the ground state wave function and displays interesting phenomena such as creation of soliton. However, this potential term leads to a nonlinear term in Schrödinger equation and make it difficult to solve analytically. This nonlinear term changes under different dimensions with the same scattering length. This paper also implements two numeric methods, time-splitting spectral method and Runge-Kutta integration. The program produces accurate simulations for both stationary and dynamic solutions to the GP equation. Meanwhile, this paper improves the accuracy of time-splitting spectral method from second-order to third-order mathematically.

## I. INTRODUCTION

Since the experimental realization of Bose-Einstein condensation (BEC) in dilute Bose gases at ultra-low temperature, there have been extensive experimental and theoretical studies on its wave-like properties. On the experimental side, one of the challenges is to engineer various magnetic traps to control BE condensate. On the theoretical side, however, one of the challenges is to model the interaction between atoms comprising the condensate. The condensate's macroscopic wave function in the limit of low temperature is well governed by the time-dependent, nonlinear Gross-Pitaevskii equation. This equation employs mean-field theory to account for the overall effect of interatomic interaction, which leads to a nonlinear term in the GP equation and complicates the solution procedure. However, a theoretical solution to the GP equation is interesting in a sense that it shows the condensate's static and dynamic properties and provides physical insight into experimental results.

Although exact solutions have already been found analytically in some restricted situations [1], the many-body Schrödinger equation in general remains unsolvable by analytical methods. Difficulty in finding analytical solutions has shifted the emphasis to numerical approximation. Over the years, many numeric techniques have been developed such as [2] for the solution to nonlinear differential equations. These techniques give display excellent agreement with experiment results [3]. Both accuracy and speed have been greatly improved at the same time. Numeric integration of the GP equation has been used to simulate the time-evolution of Bose gases in a variety of combinations of magnetic traps and atomic scattering lengths [4, 5].

There are several numerical techniques to solve the nonlinear GP equation for both stationary and dynamic

solutions. This paper mainly implements time-splitting spectral method for 1D and 2D condensates. This paper also uses Runge-Kutta integration to find stationary solutions and improve the accuracy of time-splitting technique.

In this paper, we particularly look into two situations.

- (a) 3D interacting condensate in a spherically symmetric potential
- (b) Formation and propagation of matter-wave solitons in 1D BE condensate.

The simulation program solves the ground state for 3D condensate in the spherically symmetric potential. Then we let the trapping length of the external potential oscillate with time. The the program uses the ground state as the initial wave function and simulate the condensate's dynamics in the time-dependent external potential. In the second case, the program simulates the creation process of solitons in an attractive condensate using the technique introduced in [5].

The paper has four sections. The first section derives differential equations in different situations from the nonlinear GP equation. The second section introduces the time-splitting spectral method, Runge-Kutta method, and details the process of implementing the numerical methods. The third section addressed the needs for a high-order of accuracy by improving the time-splitting methods. The last section lists the Bose gas simulations in different situations.

## II. PHYSICS OF INTERACTING BOSE-EINSTEIN CONDENSATE

To model BEC, one needs a macroscopic wave function to describe the whole system. The single-particle wave function is no longer representative of the condensate's properties and cannot reflect the atom-atom interaction among particles. To describe this many-body system, one

---

\*luocheng@grinnell.edu

needs to derive the GP equation. This paper provides a brief and non-rigorous derivation for the GP equation.

Let us start from a BE condensate consisting of  $N$  identical particles at zero temperature, and  $|\Psi\rangle$  is its state vector. Under the assumption that all particles in the condensate occupy the same ground state, the state vector could be written as

$$|\Psi\rangle = |\phi, \phi, \phi \dots \phi\rangle. \quad (\text{II.1})$$

We use  $\mathbf{r}_i$  to represent the position of the  $i$ th particle and introduce a shorthand notation,

$$\{\mathbf{r}\} = (\mathbf{r}_1, \mathbf{r}_2, \dots, \mathbf{r}_N). \quad (\text{II.2})$$

Then the macroscopic wave function  $\Psi(\{\mathbf{r}\})$  can be written as  $\langle\{\mathbf{r}\}|\Psi\rangle$ . As a Hartree mean-field ansatz, this macroscopic wave function can be written as the product of single-particle wave functions,

$$\Psi(\mathbf{r}_1, \mathbf{r}_2, \dots, \mathbf{r}_N) = \prod_{i=1}^N \phi(\mathbf{r}_i), \quad (\text{II.3})$$

with the normalization  $\int d\mathbf{r} |\phi(\mathbf{r})|^2 = 1$ .

The energy of the condensate includes the kinetic energy and potential of all particles in it and the atom-atom interaction among them. The true interparticle interaction term can be replaced by an effective delta-function potential [3]

$$U(\mathbf{r}_1, \mathbf{r}_2) = g\delta(\mathbf{r}_1 - \mathbf{r}_2), \quad (\text{II.4})$$

where  $g$  is the coupling constant, whose value depends on the dimension of the condensate.

However, this approximation to the atom-atom interaction is valid only under certain conditions [6]. First, the Bose gas is dilute so that only binary collisions are considered in the atom-atom particle. Second the characteristic particle wavelength should be much larger than

the s-wave scattering length. The second condition is also a condition for the formation of BEC and is automatically satisfied. Under these two conditions, the atom-atom interaction can be effectively replaced by a delta-function potential, whose coupling constant  $g$  depends on the s-wave scattering length.

With the effective delta-function potential, the Hamiltonian for the Bose system can be written as [7],

$$\mathcal{H} = \sum_{i=1}^N \left[ \frac{\mathbf{p}_i^2}{2m} + V(\mathbf{r}_i) \right] + g \sum_{i<j} \delta(\mathbf{r}_i - \mathbf{r}_j), \quad (\text{II.5})$$

where  $(p)_i$  is the momentum operator,  $m$  is the atomic mass,  $V(\mathbf{r}_i)$  is the external potential. From a variational perspective, the total energy can be found as

$$E = \frac{\langle\Psi|\mathcal{H}|\Psi\rangle}{\langle\Psi|\Psi\rangle}. \quad (\text{II.6})$$

In Eq. (II.6), the denominator  $\langle\Psi|\Psi\rangle$  can be expressed as

$$\langle\Psi|\Psi\rangle = \int \int d\{\mathbf{r}\} \prod |\phi(\mathbf{r}_i)|^2 = 1. \quad (\text{II.7})$$

Based on the completeness relation  $\int_{-\infty}^{\infty} d\mathbf{r} |\mathbf{r}\rangle \langle\mathbf{r}| = 1$ , the numerator in Eq. (II.6) can be written as Eq. (II.8).

$$\langle\Psi|\mathcal{H}|\Psi\rangle = \int \int \{d\mathbf{r}^{(1)}\} \{d\mathbf{r}^{(2)}\} \langle\Psi|\{\mathbf{r}^{(1)}\}\rangle \langle\{\mathbf{r}^{(1)}\}|\mathcal{H}|\{\mathbf{r}^{(2)}\}\rangle \langle\{\mathbf{r}^{(2)}\}|\Psi\rangle \quad (\text{II.8})$$

According to the structure of the Hamiltonian Eq. (II.5), the term  $\langle\{\mathbf{r}^{(1)}\}|\mathcal{H}|\{\mathbf{r}^{(2)}\}\rangle$  in the above equation can be calculated in three parts as in Eq. (II.9). For the  $i$ th particle, its kinetic energy part can be calculated as Eq. (II.10). Similarly, its external potential part can be calculated as Eq. (II.11). Finally, its interparticle interaction part is calculated as in Eq. (II.12).

$$\langle\{\mathbf{r}^{(1)}\}|\mathcal{H}|\{\mathbf{r}^{(2)}\}\rangle = \langle\{\mathbf{r}^{(1)}\}|\frac{\mathbf{p}_i^2}{2m}|\{\mathbf{r}^{(2)}\}\rangle + \langle\{\mathbf{r}^{(1)}\}|V(\mathbf{r}_i)|\{\mathbf{r}^{(2)}\}\rangle + \langle\{\mathbf{r}^{(1)}\}|g\delta(\mathbf{r}_i - \mathbf{r}_j)|\{\mathbf{r}^{(2)}\}\rangle \quad (\text{II.9})$$

$$\langle\{\mathbf{r}^{(1)}\}|\frac{\mathbf{p}_i^2}{2m}|\{\mathbf{r}^{(2)}\}\rangle = \left[ \prod_{i \neq j} \delta(\mathbf{r}_j^{(1)} - \mathbf{r}_j^{(2)}) \right] \delta(\mathbf{r}_i^{(1)} - \mathbf{r}_i^{(2)}) \left( -\frac{\hbar^2}{2m} \nabla_i^2 \right) \quad (\text{II.10})$$

$$\langle\{\mathbf{r}^{(1)}\}|V(\mathbf{r}_i)|\{\mathbf{r}^{(2)}\}\rangle = \left[ \prod_{i \neq j} \delta(\mathbf{r}_j^{(1)} - \mathbf{r}_j^{(2)}) \right] \delta(\mathbf{r}_i^{(1)} - \mathbf{r}_i^{(2)}) V(\mathbf{r}_i^{(1)}) \quad (\text{II.11})$$

$$\langle\{\mathbf{r}^{(1)}\}|g\delta(\mathbf{r}_i - \mathbf{r}_j)|\{\mathbf{r}^{(2)}\}\rangle = \left[ \prod_{k=1}^N \delta(\mathbf{r}_k^{(1)} - \mathbf{r}_k^{(2)}) \right] g\delta(\mathbf{r}_i^{(2)} - \mathbf{r}_j^{(2)}) \quad (\text{II.12})$$

$$(\text{II.13})$$

Combining the above three parts, we rewrite the numerator and further reduce it by inserting the mean-field ansatz,

$$\begin{aligned}
\langle \Psi | \mathcal{H} | \Psi \rangle &= \int \int \{d\mathbf{r}^{(1)}\} \{d\mathbf{r}^{(2)}\} \Psi(\{\mathbf{r}^{(1)}\}) \Psi(\{\mathbf{r}^{(2)}\}) \times \left[ \sum_i^N \frac{\mathbf{p}_i^2}{2m} + \sum_i^N V(\mathbf{r}_i) + \sum_{i<j}^N g\delta(\mathbf{r}_i - \mathbf{r}_j) \right] \\
&= \sum_i \int d\mathbf{r} \left\{ \phi^*(\mathbf{r}) \left( -\frac{\hbar^2}{2m} \nabla^2 \right) \phi(\mathbf{r}) + \phi^*(\mathbf{r}) V(\mathbf{r}) \phi(\mathbf{r}) \right\} + \sum_{i<j} \int d\mathbf{r} g |\phi(\mathbf{r})|^4 \\
&= N \int d\mathbf{r} \left\{ -\frac{\hbar^2}{2m} |\nabla\phi|^2 + V(\mathbf{r}) |\phi|^2 + \frac{N-1}{2} g |\phi|^4 \right\} \tag{II.14}
\end{aligned}$$

Let the macroscopic wave function be  $\psi(\mathbf{r}) = \sqrt{N}\phi(\mathbf{r})$ . Since the denominator Eq. (II.7) is 1, by replacing single-particle wave function  $\phi$  by the condensate wave function  $\psi$ , we can write the energy functional as

$$\begin{aligned}
E[\phi] &= \int d\mathbf{r} \left\{ -\frac{\hbar^2}{2m} |\nabla\psi|^2 + V(\mathbf{r}) |\psi(\mathbf{r})|^2 + \frac{1}{2} N g |\psi(\mathbf{r})|^4 \right\}. \tag{II.15}
\end{aligned}$$

At the same time, the condensate wave function  $\psi$  also relates to the number of particle

$$\int d\mathbf{r} |\psi(\mathbf{r})|^2 = N[\psi] \tag{II.16}$$

Both functionals, Eq. (II.15) and Eq. (II.16) must be satisfied by writing

$$\delta E - \mu \delta N = 0, \tag{II.17}$$

where  $\mu$  is chemical potential. Since  $\mu$  is fixed condensate, Eq. (II.17) can be expressed as  $\delta(E - \mu N)$ , which we need to extremize to derive the GP equation.

Let  $f[\psi]$  represent  $E - \mu N$ . Then  $\delta f[\psi]$  can be written as

$$\begin{aligned}
\delta f[\psi] &= \delta \int d\mathbf{r} \left[ -\frac{\hbar^2}{2m} |\nabla\psi|^2 + (V(\mathbf{r}) - \mu) |\psi|^2 + \frac{U_0}{2} |\psi|^4 \right] \\
&= 2\delta\psi \int d\mathbf{r} \psi \left[ -\frac{\hbar^2}{2m} \nabla^2 + V(\mathbf{r}) - \mu + N g |\psi|^2 \right]. \tag{II.18}
\end{aligned}$$

The variation of  $f[\psi]$  with respect to  $\psi$  is required to be stationary,  $\frac{\partial f}{\partial \psi} = 0$ , which then can be reduced to the time-independent GP equation,

$$\mu\psi(\mathbf{r}) = \left[ -\frac{\hbar^2}{2m} \nabla^2 + V(\mathbf{r}) + N g |\psi(\mathbf{r})|^2 \right] \psi(\mathbf{r}). \tag{II.19}$$

As mentioned in the beginning, the derivation here is only a short treatment of the interacting many-body system. Although this paper derives the GP equation under certain assumptions like the Hartree mean-field ansatz, this equation is still valid in more general case and a rigorous derivation can be found at Ref. [8].

### III. NONLINEAR GROSS-PITAEVSKII EQUATION

In the last section, we show that at zero temperature the Bose-Einstein condensate is well modeled by a macroscopic wave function and derive the time-independent GP equation. The time-dependent wave function,  $\Psi(\mathbf{r}, t)$ , can be obtained from the time-dependent GP equation:

$$i\hbar \frac{\partial \Psi(\mathbf{r}, t)}{\partial t} = \left[ -\frac{\hbar^2}{2m} \nabla^2 + V(\mathbf{r}) + N g |\Psi(\mathbf{r}, t)|^2 \right] \Psi(\mathbf{r}, t), \tag{III.1}$$

with the normalization  $\int |\Psi(\mathbf{r}, t)|^2 d\mathbf{r} = 1$ .

#### A. Dimensionless GPE for simple harmonic oscillator

The 3D simple harmonic oscillator can be written as  $V(\mathbf{r}) = \frac{1}{2} m (\omega_x^2 x^2 + \omega_y^2 y^2 + \omega_z^2 z^2)$ . We are going to make the following change to the parameters

$$\tilde{t} = \omega_x t \quad \tilde{\mathbf{r}} = \frac{\mathbf{r}}{a_{ho}} \quad \tilde{\Psi}(\tilde{\mathbf{r}}, \tilde{t}) = a_{ho}^{3/2} \Psi(\mathbf{r}, t), \tag{III.2}$$

where  $a_{ho}$  is the harmonic oscillator length,  $\sqrt{\frac{\hbar}{m\omega_x}}$ . And the coupling constant is [3]

$$g_{3D} = \frac{4\pi\hbar^2 a_s}{m}, \tag{III.3}$$

where  $a_s$  is the s-wave scattering length. After inserting Eqs. (III.2) into the GP equation, Eq. (III.1) can be transformed to a dimensionless GP equation

$$i \frac{\partial \tilde{\Psi}(\tilde{\mathbf{r}}, \tilde{t})}{\partial \tilde{t}} = \left[ -\frac{1}{2} \tilde{\nabla}^2 + \tilde{V}(\tilde{\mathbf{r}}) + k_{3D} |\tilde{\Psi}(\tilde{\mathbf{r}}, \tilde{t})|^2 \right] \tilde{\Psi}(\tilde{\mathbf{r}}, \tilde{t}), \tag{III.4}$$

where

$$\tilde{V}(\tilde{\mathbf{r}}) = \frac{1}{2} (\tilde{x}^2 + \gamma_y^2 \tilde{y}^2 + \gamma_z^2 \tilde{z}^2), \tag{III.5}$$

and

$$\begin{aligned}
\gamma_y &= \frac{\omega_y}{\omega_x} & \gamma_z &= \frac{\omega_z}{\omega_x} \\
k_{3D} &= \frac{N g_{3D}}{a_{ho}^3 \hbar \omega_x} = \frac{4\pi N a_s}{a_{ho}} \tag{III.6}
\end{aligned}$$

Similarly, the dimensionless 1D GP equation could be expressed as

$$i \frac{\partial \tilde{\Psi}(\tilde{x}, \tilde{t})}{\partial \tilde{t}} = \left[ -\frac{1}{2} \frac{\partial^2}{\partial \tilde{x}^2} + \tilde{V}(\tilde{x}) + k_{1D} \left| \tilde{\Psi}(\tilde{x}, \tilde{t}) \right|^2 \right] \tilde{\Psi}(\tilde{x}, \tilde{t}), \quad (\text{III.7})$$

where  $k_{1D} = Ng_{1D}$ . The only difference is the coupling constant, whose values depends on the BEC's dimension. In the soliton-creation simulation in this paper, the renormalized quasi-1D coupling constant is  $g_{1D} = 2a_s \omega \rho \hbar$  [9].

### B. BE condensate in 3D spherically symmetric potential

One of our question is to simulate a 3D condensate in a spherically symmetric potential, which can be perfectly described a 1D GP equation. The external potential term is given as

$$V(\mathbf{r}) = \frac{1}{2} m \omega^2 r^2, \quad (\text{III.8})$$

where  $\omega$  is the angular frequency and  $r$  is the radial distance. We break the wave function  $\Psi$  into a time-dependent piece and a time-independent piece,

$$\Psi(\mathbf{r}, t) = \exp\left(-\frac{i\mu t}{\hbar}\right) \psi(\mathbf{r}). \quad (\text{III.9})$$

Since the external potential is spherically symmetric,  $\psi$  has a constant angular component and can be written as

$$\frac{1}{\sqrt{4\pi}} R(r). \quad (\text{III.10})$$

Now we introduce a notation that  $y(r) = rR(r)$ . Then the GP equation Eq. (III.1) can be transformed to

$$\left[ -\frac{\hbar^2}{2m} \frac{\partial^2}{\partial r^2} + \frac{1}{2} m \omega^2 r^2 + \frac{Ng_{3D}}{4\pi} \left| \frac{y(r)}{r} \right|^2 \right] y(r) = \mu y(r), \quad (\text{III.11})$$

where  $\mu$  is the chemical potential. The above GP equation can be also made dimensionless with the technique introduced in the previous sub-section. The dimensionless GP equation for spherical potential is very similar to a pure 1D GP equation Eq. (III.7). We can use our 1-D simulation to solve for  $y(r)$  as long as we can find the relation between  $y(r)$  and the 1-D wave function,  $\psi_{1D}$ . We can find this relation by comparing their normalizations. Because  $\psi^{3D}$  is normalized to 1, the normalization of  $y(r)$  is

$$\int_0^\infty dr |y(r)|^2 = 1. \quad (\text{III.12})$$

In the 1-D case,  $\int_{-\infty}^\infty dx |\psi^{1D}(x)|^2 = 1$ . Because  $\psi^{1D}$  is symmetric about the origin, the normalization condition can be written as

$$\int_0^\infty dx |\psi^{1D}|^2 = \frac{1}{2}. \quad (\text{III.13})$$

Therefore,  $y(r)$  and  $\psi^{1D}(x)$  have to satisfy

$$y(r) = \sqrt{2} \psi^{1D}(x) \quad (\text{III.14})$$

If we insert Eq. (III.14) into the nonlinear term in Eq. (III.11), the 1-D coupling constant is doubled

$$k_{1D} = 2 \frac{k_{3D}}{4\pi}. \quad (\text{III.15})$$

Since  $y(r)$  goes to zero when  $r$  gets close to zero, the pure 1-D solution,  $\psi^{1D}(x)$ , has to satisfy the boundary condition that  $\psi(0) = 0$ . Therefore, the ground state of 3-D spherically symmetric case is the first-excited state in a pure 1-D situation.

## IV. NUMERIC TECHNIQUES

Mainly, we use time-splitting spectral method(TSSP) to simulate BEC described by the GP equation [4]. The basic idea of TSSP is that the wave function at certain time can be calculated by integrating the time-evolution operator iteratively over time. With the help of computer, such vast amount of computation work can be done within several minutes while remaining a high degree of accuracy. Besides solving time-evolution problems, TSSP also enables us to find ground state wave functions in different potential through a technique called imaginary time propagation [10]. In addition to TSSP, this paper also implements Runge-Kutta method to obtain stationary solutions to time-independent GP equation. Only at eigenvalues, wave functions decays to zero when distance approaches infinite. We use Bode's eight-point rule to normalize the wave function [11].

First the wave function is discretized in time and space. The program is fed with an initial wave function found by imaginary time propagation. Through the time-evolution operator, one can calculate the wave function at any later time in terms of the initial wave function. By keeping the mesh size and time step sufficiently small, the results are shown to be very accurate and stable. Each time step is divided into three sub-steps. Two sub-steps involve the change caused by external potential and interatomic interaction. The other one includes the spatial derivative. As long as the boundary conditions for infinite potential well are satisfied, the spectral method is valid.

### A. Time-splitting spectral method

The essential mechanism in TSSP is to propagate the wave function via the time-evolution operator, which can be usually written as

$$\mathcal{U}(t, t + dt) = \exp\left(-\frac{i}{\hbar} \mathcal{H} dt\right), \quad (\text{IV.1})$$

where  $\mathcal{H}$  is the Hamiltonian of Eq. (III.1) [12]. The wave function after an infinitesimal time interval  $dt$  is

$$\Psi(\mathbf{r}, t + dt) = \mathcal{U}(t, t + dt)\Psi(x, t). \quad (\text{IV.2})$$

Eq. (III.1) can be re-written as

$$i\hbar \frac{\partial \Psi(\mathbf{r}, t)}{\partial t} = \mathcal{H}\Psi(x, t). \quad (\text{IV.3})$$

The solution to Eq. (IV.3) can be expressed as  $\Psi(\mathbf{r}, t) = T(t)\psi(\mathbf{r})$ . In the case where  $\mathcal{H}$  is time-independent,  $\mathcal{U}$  is expressed as Eq. (IV.1). In the case where  $\mathcal{H}$  is time-dependent, the time evolution operator can be expressed as Dyson series, given in Eq. (V.1) [12]. In a low-order approximation method, the time-dependent Hamiltonian can still be expressed as Eq. (IV.1). A high-order approximation using Dyson series is discussed in the next section. By integrating this time-evolution operator repeated, the simulation program can produce the wave function at any desired time point with an input of initial state.

The stationary solution to GP equation can be obtained by imaginary time propagation using time-evolution operator. The root-finding process can start with any wave function as long as it has the ground state component. A rigorous mathematic investigation shows that when a wave function propagates in imaginary time, the coefficients of high energy states decreases faster than those of low energy states. Therefore, the imaginary time propagation can highlight and, ultimately, select the ground state wave function given sufficiently long time.

Let  $|\Psi\rangle$  represent the initial state, which can break down into a linear combination of eigenstates in momentum space,

$$\begin{aligned} \Psi(\mathbf{r}, t) &= \hat{\mathbf{r}}|\Psi\rangle \\ |\Psi\rangle &= \sum_{m=1}^N C_m |p_m\rangle, \end{aligned} \quad (\text{IV.4})$$

where  $N$  is the number of basic states in the given region,  $|p_i\rangle$  is an eigenket of the *momentum operator*  $\hat{p}$ , i.e. a basket of the momentum space. Eigenvalue  $E_m$  would be the energy at the eigenket,  $|p_m\rangle$ . After an infinitesimal interval in imaginary time  $-i d\mu$ , the initial state becomes

$$\begin{aligned} \mathcal{U}|\Psi\rangle &= \sum_{m=1}^N C_m \mathcal{U}|p_m\rangle \\ &= \sum_{m=1}^N C_m \exp\left(-\frac{E_m}{\hbar} d\mu\right) |p_m\rangle. \end{aligned} \quad (\text{IV.5})$$

The new coefficient for eigenket  $|p_m\rangle$  becomes

$$C'_m = \exp\left(-\frac{E_m}{\hbar} d\mu\right) C_m. \quad (\text{IV.6})$$

Therefore, the coefficients undergo an exponential decay. More importantly, a higher energy state leads to a

greater shrinking factor of its coefficient. In the long-run, the low-energy state, especially ground state, will finally stand out as the dominant component of the whole wave function.

There are several methods to calculate the time-evolution operator. This paper uses time-splitting spectral method, which uses Strang Splitting to split  $\mathcal{U}$  [4] and the spectral method to calculate kinetic energy [2]. The full Hamiltonian is broken into a non-derivative part and a derivative one:

$$\mathcal{H} = \mathcal{H}_1 + \mathcal{H}_2, \quad (\text{IV.7})$$

where

$$\begin{aligned} \mathcal{H}_1 &= V(\mathbf{r}) + g|\Psi(\mathbf{r}, t)|^2 \\ \mathcal{H}_2 &= -\frac{\hbar^2}{2m}\nabla^2. \end{aligned} \quad (\text{IV.8})$$

Strang splitting technique gives a second-order accuracy approximation. Other high-order splitting methods are also available for higher accuracy. However, here the time-evolution operator only has a second-order of accuracy. There is no need to utilize other high-order splitting methods. Under Strang splitting scheme, the time-evolution operator could be expressed as,

$$\begin{aligned} \mathcal{U}_0(dt) &= \\ &= \exp\left(-\frac{i\mathcal{H}_1}{\hbar} \frac{dt}{2}\right) \exp\left(-\frac{i\mathcal{H}_2}{\hbar} dt\right) \exp\left(-\frac{i\mathcal{H}_1}{\hbar} \frac{dt}{2}\right) + \mathcal{O}(dt^2). \end{aligned} \quad (\text{IV.9})$$

$\mathcal{H}_1$  is diagonal in coordinate space and  $\mathcal{H}_2$  is diagonal in momentum space. Therefore, the whole integration of Hamiltonian is calculated conveniently by three sub-steps: first half time step by  $\mathcal{H}_1$ , then full time step by  $\mathcal{H}_2$ , and finally half time step by  $\mathcal{H}_1$ . The calculation of  $\mathcal{H}_1$  is straightforward because both the external potential and atomic interaction are scalars. To calculate the kinetic energy part  $\mathcal{H}_2$ , the simulation first uses Fourier transformation to convert the wave function from real space space to moment space, and then uses spectral methods to calculate the coefficient changes for each eigenfunction as in Eq. (IV.5).

The detailed formula of integration in 1D situation is given as the following.

After the half time step for  $\mathcal{H}_1$ ,

$$\begin{aligned} \Psi^* &= \exp\left[-\frac{i\mathcal{H}_1}{\hbar} \frac{dt}{2}\right] \Psi(x, t) \\ &= \exp\left[-\frac{idt}{2\hbar} (V(x) + g|\Psi(x, t)|^2)\right] \Psi(x, t). \end{aligned} \quad (\text{IV.10})$$

After the full time step for  $\mathcal{H}_2$ ,

$$\begin{aligned} \Psi^{**}(x) &= \exp\left[-\frac{i\mathcal{H}_2}{\hbar} dt\right] \Psi^*(x) \\ &= \frac{1}{N} \sum_{m=-\frac{N}{2}+1}^{N/2} \exp\left(-\frac{iE_m}{\hbar} dt\right) C_m \exp\left(\frac{ip_m}{\hbar} x\right), \end{aligned} \quad (\text{IV.11})$$

where  $N$  is the number of points,  $p_m$  is the  $m$ th eigenfunction, and  $C_m$  the corresponding coefficient. Coefficient of each eigenfunction can be calculated through Fourier transformation [13],

$$C_m = \int_{-\infty}^{\infty} dx \exp\left(-\frac{ip_m x}{\hbar}\right) \Psi^*(x). \quad (\text{IV.12})$$

After the last half time step for  $\mathcal{H}_1$ ,

$$\begin{aligned} \Psi(x, t + dt) &= \exp\left(-\frac{i\mathcal{H}_2 dt}{\hbar}\right) \Psi^{**}(x) \\ &= \exp\left[-\frac{idt}{2\hbar} (V_{ext}(x) + g|\Psi(x, t)|^2)\right] \Psi^{**}(x) \end{aligned} \quad (\text{IV.13})$$

The generalization from 1D to 2D code is straightforward. We use tensor product of wave functions along  $x$  and  $y$  directions and 2-dimension Fourier transformation. Besides time-splitting spectral method, Crank-Nicholson difference rule could also be used to calculate the time-evolution operator [14].

## B. Runge-Kutta method

The main idea of the Runge-Kutta method is to integrate the wave function at different energies, and if the energy tried is the eigenvalue, the wave function decays exponentially as  $x$  goes to infinity. The Runge-Kutta method only solves the time-independent 1D Schrödinger equation. For convenience, we use  $y$  to represent the wave function,  $\psi$ . The time-independent GP equation, Eq. (II.19), can be transformed to

$$\begin{aligned} y'' &= -k(x, y)^2 y \\ k(x, y) &= \sqrt{\frac{2m}{\hbar^2} (E - V(x) - g_{1D} |y|^2)}. \end{aligned} \quad (\text{IV.14})$$

If we treat  $y$  and  $y'$  as two individual functions,  $y''$  can be treated as the first derivative of  $y'$ . Let us make a vector  $\mathbf{y} = \begin{bmatrix} y \\ y' \end{bmatrix}$ . Then using Eq. (IV.14), the derivative of the new state vector,  $\mathbf{y}'$  which can be expressed  $\begin{bmatrix} y' \\ y'' \end{bmatrix}$ , can be represented as a function of  $x$  and  $\mathbf{y}$

$$\mathbf{y}' = \begin{bmatrix} y' \\ y'' \end{bmatrix} = f(x, \mathbf{y}) = \begin{bmatrix} y' \\ -k(x)^2 y \end{bmatrix}. \quad (\text{IV.15})$$

We treat  $\mathbf{y}(x)$  as a function of  $x$  and then the Runge-Kutta equations look like

$$\begin{aligned} \mathbf{k}_1 &= hf(x_n, \mathbf{y}_n) \\ \mathbf{k}_2 &= hf\left(x_n + \frac{h}{2}, \mathbf{y}_n + \frac{\mathbf{k}_1}{2}\right) \\ \mathbf{k}_3 &= hf\left(x_n + \frac{h}{2}, \mathbf{y}_n + \frac{\mathbf{k}_2}{2}\right) \\ \mathbf{k}_4 &= hf(x_n + h, \mathbf{y}_n + \mathbf{k}_3), \end{aligned} \quad (\text{IV.16})$$

and then the wave function at next position point can be expressed as

$$\mathbf{y}_{n+1} = \mathbf{y}_n + \frac{\mathbf{k}_1}{6} + \frac{\mathbf{k}_2}{3} + \frac{\mathbf{k}_3}{3} + \frac{\mathbf{k}_4}{6} + \mathcal{O}(h^5) \quad (\text{IV.17})$$

The Runge-Kutta integration starts from two points, one at the origin and the other at the boundary. When the system's energy happens to be the eigenvalue, these two parts of the wave functions is a continuous at the previously-selected position, that is,

$$\frac{\psi_1(x)}{\psi_1'(x)} = \frac{\psi_2(x)}{\psi_2'(x)} \quad (\text{IV.18})$$

For the start point at the origin, the initial conditions should have a reasonable positive value and zero position derivative. Since the wave function shall decay exponentially along the  $x$ -axis, the initial conditions for the start point at the boundary should have a small positive value for wave function and a small negative positive derivative.

## V. HIGH-ORDER SPLIT-OPERATOR METHOD

The accuracy of the time-splitting spectral method partially depends on how the time-evolution operator is approximated and the time-splitting method. In a low-order accuracy simulation,  $\mathcal{H}$  is assumed to be constant over the time step  $\Delta t$ , which has the first-order of accuracy, i.e., the error in  $\Psi(t + \Delta t)$  is  $\Delta t^2$ . In a real world physical system, the Hamiltonian will not remain constant and this low-order approximation introduces a considerable degree of inaccuracy. In [15], the approximation to the time-evolution operator is improved to second-order accuracy by including the first-order time-derivative of  $\mathcal{H}$ . In the following section, we will improve the approximation to the third-order. Although the third-order approximation requires one to include the second order derivative of  $\mathcal{H}$  and need extra memory to store the wave function at previous time points, this high-order approximation may prove useful in a complicated and dynamic many-body system.

For time-dependent Hamiltonian, the time-evolution operator can be expressed as the sum of terms in the Dyson series [12]

$$\begin{aligned} \mathcal{U}(t_0, t) &= \\ &= 1 + \sum_{n=1}^{\infty} \left[ \left(-\frac{i}{\hbar}\right)^n \int_{t_0}^t dt_1 \int_{t_0}^{t_1} dt_2 \cdots \int_{t_0}^{t_{n-1}} dt_n \prod_{i=1}^n \mathcal{H}(t_i) \right]. \end{aligned} \quad (\text{V.1})$$

We let  $t = t_0 + \Delta t$  and  $\tilde{H}^{(i)}(t)$  denote the  $i$ th derivative of  $\tilde{H}$  at time  $t$ . By rigorous mathematic transformation, the Dyson series can be approximated to the third-order

of accuracy by

$$\begin{aligned} \mathcal{U}(t_0 + \Delta t, t_0) &= 1 + \frac{\mathcal{H}(t_0)}{i\hbar} dt \\ &+ \left[ \frac{1}{2} \frac{\mathcal{H}^{(1)}(t_0)}{i\hbar} + \frac{1}{2} \left( \frac{\mathcal{H}(t_0)}{i\hbar} \right)^2 \right] dt^2 \\ &+ \left[ \frac{1}{6} \frac{\mathcal{H}^{(2)}}{i\hbar} + \frac{1}{2} \left( \frac{1}{i\hbar} \right)^2 \mathcal{H}(t_0) \mathcal{H}^{(1)}(t_0) + \frac{1}{6} \left( \frac{\mathcal{H}(x)}{i\hbar} \right)^3 \right] dt^3 \\ &+ \mathcal{O}(dt^4) \end{aligned} \quad (\text{V.2})$$

Now we approximate the new series by a function

$$\mathcal{U}(t_0, t_0 + dt) = \exp \left[ -\frac{i}{\hbar} (\mathcal{H}(t_0) dt + F(dt)) \right], \quad (\text{V.3})$$

where  $F(dt)$  is the function we want to find that can equalize Eq. (V.3) to third-order of accuracy Dyson series Eq. (V.2). By expanding Eq. (V.3) in Taylor series, we find that

$$F(dt) = \frac{1}{2} \mathcal{H}^{(1)}(t_0) dt^2 + \frac{1}{3} \mathcal{H}^{(2)} dt^3. \quad (\text{V.4})$$

Only the potential component in Hamiltonian changes over the time  $dt$  while the kinetic energy component,  $T$ , remains constant. Therefore, we write  $\tilde{V}(t_0)$  as our new potential term and Hamiltonian becomes

$$\begin{aligned} \mathcal{H}(t_0) &= T + \tilde{V}(t_0) \\ \tilde{V}(t_0) &= \frac{1}{12} [23V(t_0) - 16V(t_0 - dt) + 5V(t_0 - 2dt)] \end{aligned} \quad (\text{V.5})$$

To match the third-order of accuracy of the Hamiltonian, we also need to improve the time-split operator method to the same order of accuracy. From Ref. [16], we can express the new time-evolution operator as the following

$$\begin{aligned} \mathcal{U}(t, t + dt) &= \\ &\mathcal{U}(t, t + \lambda dt) \mathcal{U}(t, t + (1 - 2\lambda dt)) \mathcal{U}(t, t + \lambda dt) \\ &+ C [2\lambda^3 + (1 - 2\lambda)^3] dt^3 + \mathcal{O}(dt^4) \end{aligned} \quad (\text{V.6})$$

where  $C$  is a constant and  $\lambda$  is a parameter. By making the coefficient of  $dt^3$  vanish, we can improve the split-operator method to the third-order of accuracy. We solve for  $\lambda$  in the equation

$$\lambda^3 + (1 - 2\lambda)^3 = 0 \quad (\text{V.7})$$

and get  $\lambda = \frac{1}{2 - \sqrt[3]{2}}$ .

An even-higher order of accuracy could be obtained by including a further term in Dyson series. However, the split-operator method needs to split each time step into even smaller sub-steps and involves more Fourier transformation in each cycle. More computation thus are required to gain such high accuracy. Some paper has already discussed which splitting method will be most efficient [17]. However, in this paper, high-order accuracy could still be obtained by making each time step size smaller and integrate for more times.

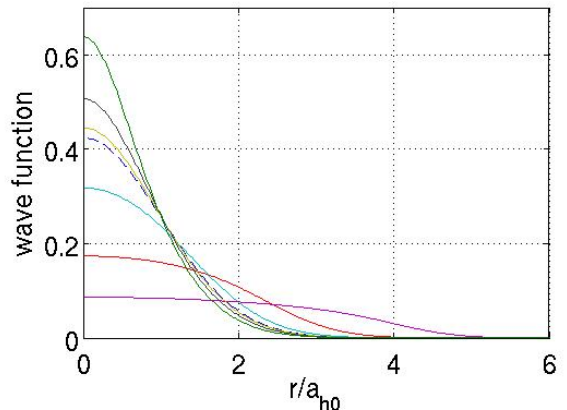


FIG. 1: ground state wave functions for condensates in a spherically symmetric potential. The dashed data line is the wave function for the ideal Bose gas. The plots from the top to bottom are wave functions for  $\frac{Na}{a_{ho}} = -0.5, -0.3, -0.1, 1, 10, 100$ , from attractive to repulsive. The whole wave function is normalized to 1.

## VI. APPLICATIONS

In this paper, most of the simulations use TSSP because it is faster and more versatile than Runge-Kutta method. ground state wave functions, found by imaginary time propagation, are fed into TSSP as the initial wave function. Computer simulations display the dynamics of BE condensates after the external potential or the coupling constant has changed.

### A. 3D Spherically symmetrical potential

#### 1. Ground state

We test our time-splitting spectral method on the 3D gas in a spherically symmetrical potential. With Eq. (III.11), we can model this special 3D condensate using our 1D code. And the 1D simulation yields satisfactory plots of the ground states of the condensate under different coupling constants, which matches the numeric results in Dalfovo's paper.

We tried  $\frac{Na}{a_{ho}} = -0.2, -0.5, -0.6$  for the attractive interaction and  $\frac{Na}{a_{ho}} = 1, 10, 100$  for the repulsive interaction. The x-grid range is 0 to 6 with 1024 data points. The time step is -0.0001i for the imaginary time relaxation, repeated for 50,000. Although we could make a more precise simulation of the ground states, the above configuration is already producing accurate results compared to Dalfovo's paper.

The whole simulation is very efficient, taking less than 1 minutes to complete. The initial wave function is the

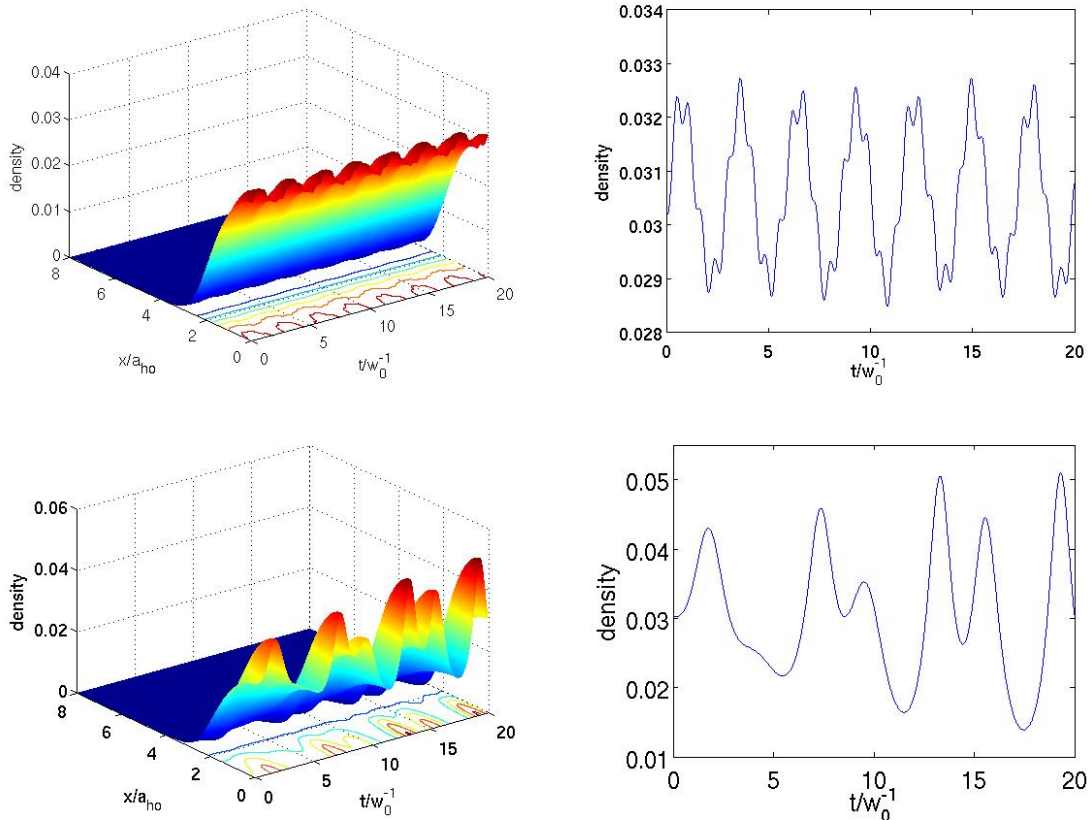


FIG. 2: Brezing mode

first excited state in a pure 1D simple harmonic potential

$$\Psi(r, 0) = \frac{1}{\sqrt[4]{\pi}} \sqrt{2r} \exp\left(-\frac{r^2}{2}\right). \quad (\text{VI.1})$$

Results are shown in Fig. (1).

## 2. Time-dependent oscillator potential

The condensate enters the Brezing mode when either the external potential or the coupling constant changes. Here we let the strength of the external potential change with time. The external potential term in the dimensionless GP equation Eq. (III.7) is

$$V(r, t) = \frac{1}{2} r^2 (1 + A \sin(kt))^2, \quad (\text{VI.2})$$

where  $A$  is the amplitude, the percent of change and  $k$  describes how fast the potential changes.

First we find the ground state wave function in each potential by imaginary time propagation. The initial wave function fed into the program is the ground state for the ideal gas in a simple harmonic oscillator,

$$\Psi(r, 0) = \frac{1}{\sqrt[4]{4\pi}} \exp\left(-\frac{x^2}{2}\right). \quad (\text{VI.3})$$

Next, the external potential starts to vary with time and we are interested in how different parameters will affect the collective oscillation of the condensate in an oscillatory potential such as stability and periodicity.

## B. Creation of solitons

Solitons have always been a popular subject of mathematical and physics research. They occur in various physics systems ranging from water to light, and have wide applications because of its stability. Recent BEC experiments have successfully created solitons in this nonlinear many-body system via various techniques [18, 19]. Here we use the method introduced in Ref. ([5]) to create solitons in attractive BEC. First a repulsive BEC is created in a trapping potential. Next, the external potential is flipped to be repulsive and the scattering length is to attractive. If parameters satisfy certain criteria, the condensate separates out a chain of well localized wave packet. We also let the created solitons enter a “flat” region, and study the conditions under which these solitons remain stable.

We simulate the creation process with our 1D code. The coupling constant The initial wave function fed into

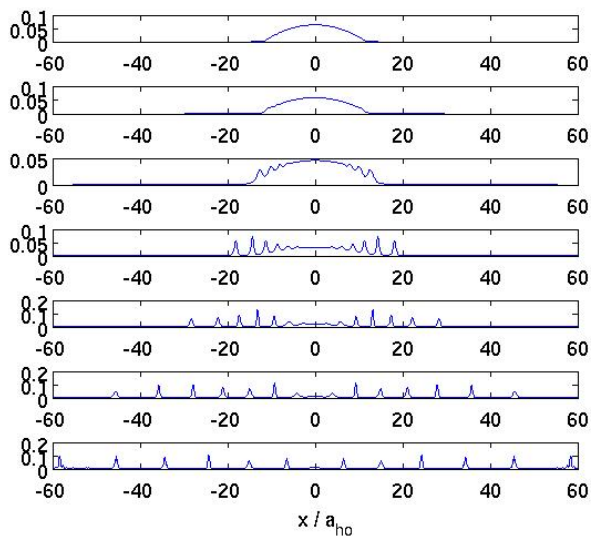


FIG. 3: creation of solitons

the simulation program is the ground state in a simple harmonic First, we find the ground state by repeating time step,  $dt = -0.001i$  by 50,000 times. Results are shown in Fig. (VIB).

## VII. CONCLUSION

In this paper, we have shown that BEC can be modeled by the nonlinear GP equation. First, we use the mean-field theory to account for the atom-atom interac-

tion and provide a brief derivation of the GP equation. Second, the paper transforms the GP equation to a dimensionless form and explore its different forms in different situations including spherically symmetric potential and soliton-creation. However, the nonlinearity of the atom-atom interaction makes the GP equation hard to solve analytically. Instead, with the help of computer, we are able to approximate the solutions numerically. We have obtained accurate results for both stationary and time-evolution problems, and have found good agreement with other paper's results, proving the validity of our codes. In the last section, we apply our working simulation codes to two situations we are interested. However, we have not performed a comprehensive study of the physics behind the dynamics of the interacting Bose gases in these two situations.

During the research process, we met more problems than we solved. One of the ventures of future work involves improving our understanding of the different regimes in 1D dilute gases. The mean-field theory underlying GP equation is valid in 3D experiments. However, in the low dimensional system, the many-body system might be well-represented by the mean-field. The delta-function potential becomes a poor approximation to the true atom-atom interaction. In Ref. ([20]), it is pointed out that in the low-dimensional regime, the GP equation needs a fundamental modification and the power of the nonlinear term also needs to change. A more rigorous and comprehensive discussion can be found at Ref. ([21]) However, because of the complexity of the BEC system, the discussion still has not reached an universal agreement. A solid mathematical exploration of situations beyond mean-field theory is needed for future study on the low-dimensional BEC.

- 
- [1] E. H. Lieb and W. Liniger, Phys. Rev. **130** (1963).
  - [2] M. D. Feit, J. J. A. Fleck, and A. Steiger, J. Comput. Phys. **47**, 412 (1982).
  - [3] F. Dalfovo, S. Giorgini, L. Pitaevskii, and S. Stringari, Rev. Mod. Phys. **71**, 463 (1999).
  - [4] W. Bao, D. Jaksch, and P. A. Markwich, J. Comput. Phys. **187**, 318 (2003).
  - [5] L. D. Carr and J. Brand, Phys. Rev. A **70**, 033607 (2004).
  - [6] A. Leggett, Rev. Mod. Phys. **73**, 307 (2001).
  - [7] C. J. Pethick and H. Smith, *Bose-Einstein Condensation in Dilute Gases* (Cambridge University Press, 2002).
  - [8] E. H. Lieb, R. Seiringer, and J. Yngvason, Phys. Rev. A **61**, 043602 (2000).
  - [9] L. Carr and Y. Castin, Phys. Rev. A **66**, 63602 (2002).
  - [10] N. Parker, *Numerical Studies of Vortices and Dark Solitons in Atomic Bose-Einstein Condensates* (2004).
  - [11] M. Abramowitz and I. A. Stegun, *Handbook of mathematical functions, with formulas, graphs and Mathematical* (US Govt. Print. Off., 1964).
  - [12] J. J. Sakurai, *Modern Quantum Mechanics* (Addison-Wesley Publishing Company, 1994).
  - [13] D. Brandwood, *Fourier Transform in Radar and Signal Processing* (unkonw, 000).
  - [14] W. H. Press, S. A. Teukolsky, W. T. Vetterling, and B. P. Flannery, *Numerical Recipes in Fortran: The Art of Scientific Computing* (Cambridge University Press, 1992).
  - [15] B. Jackson and E. Zaremba, Phys. Rev. A **66**, 033606 (2002).
  - [16] A. D. Bandrauk and H. Shen, Can. J. Chem. **70** (1992).
  - [17] M. Thalhammer, M. Caliari, and C. Neuhauser, J. Comput. Phys. **228**, 822 (2009).
  - [18] B. Anderson and M. Kasevich, Science **282**, 1686 (1998).
  - [19] K. Strecker, G. Partridge, A. Truscott, and R. Hulet, Nature **417**, 150 (2002).
  - [20] E. B. Kolomeisky, J. P. S. T. J. Newman, and X. Qi, Phys. Rev. Lett. **85**, 1146 (2000).
  - [21] E. H. Lieb, R. Seiringer, and J. Yngvason, Commun. Math. Phys. **244**, 347 (2004).